LOCAL FERMI GAS IN INCLUSIVE MUON CAPTURE FROM NUCLEI* **

J.E. Amaro, J. Nieves, M. Valverde

Departamento de Física Atómica, Molecular y Nuclear, Universidad de Granada
18071 Granada, Spain

C. Maieron

INFN, Sezione di Catania, Via Santa Sofia 64, 95123 Catania, Italy

(Received June 19, 2006)

We compare local Fermi gas and shell model in muon capture in nuclei in order to estimate the effect of finite nuclear size in low energy weak reactions.

PACS numbers: 23.40.Bw, 25.30.–c, 21.60.Cs

1. Introduction

In this paper we study the importance of nuclear finite size effects in inclusive muon capture reactions. The inclusive muon capture process in nuclei

$$\mu^- + {}^A_Z X \to X + \nu_\mu \,, \tag{1}$$

is very similar to neutrino scattering off nuclei

$$\nu_\mu + {}^A_Z X \to X + \mu^- \tag{2}$$

and is experimentally more accessible so it serves as a benchmark for testing theoretical models of the latter process.

The motivation for this investigation comes from the results of a model (published in [1]), which describes rather well inclusive $^{12}\mathrm{C}(\nu_\mu, \mu^-)X$ and $^{12}\mathrm{C}(\nu_e, e^-)X$ cross sections near threshold and inclusive muon capture by

* Presented by M. Valverde at the XX Max Born Symposium "Nuclear Effects in Neutrino Interactions", Wrocław, Poland, December 7–10, 2005.

** This work was supported by DGI and FEDER funds, contracts BFM2005-00810 and BFM2003-00856 and by the Junta de Andalucía (FQM-225).

nuclei. This approach, which is an extension of the quasi–elastic (QE) inclusive electron scattering model of [2], is based on a Local Fermi Gas (LFG), where the simplicity of the model makes it possible to include a great variety of effects into the reaction dynamics. The goal of this paper is to investigate whether finite nucleus effects that are not addressed by a LFG can affect significantly the results of the model in [1].

There already exist microscopic calculations of neutrino–nucleus reactions and muon capture that treat correctly the finite size of the system. However, there are some dynamical issues that are implemented in a different fashion in a LFG model so a direct comparison of these models is not possible and we can not extract the effect of the inclusion of nuclear structure details. For this reason, we perform a comparison of the LFG model with a extreme shell model (SM), *i.e.* single particle states in a Woods–Saxon (WS) potential, where the finite size effects can be easily recognized.

In the second section we will introduce the model of [1] as applied to inclusive nuclear muon capture and give some numerical results to be compared with experiment. Then we will introduce the extreme SM and a simplified LFG model. In the fourth section we will show the comparison between the two models. We will finish with some conclusions.

More details on this issue can be found in [3]. A more comprehensive analysis of the uncertainties in the model of [1] can be found in [4].

2. Inclusive muon capture in nuclei

The evaluation of the decay width for inclusive muon capture in finite nuclei proceeds in two steps. In the first one we evaluate the spin averaged decay width for a muon at rest in a Fermi sea of protons and neutrons $\hat{\Gamma}\left(\rho_p, \rho_n\right)$ with $N \neq Z$. In the second step, we use the LFG approximation to go to finite nuclei and evaluate

$$\Gamma = \int d^3\boldsymbol{r} |\phi_{1\mathrm{s}}(\boldsymbol{r})|^2 \, \hat{\Gamma}\left(\rho_p(r), \rho_n(r)\right) \, , \tag{3}$$

where $\phi_{1s}(\vec{r}\,)$ is the muon wave function in the $1s$ state from where the capture takes place. It has been obtained by solving the Schrödinger equation with a Coulomb interaction taking into account the finite size of the nucleus and vacuum polarization. This approximation assumes a zero range of the interaction, that becomes highly accurate as long as the $\vec{q}$ dependence of the interaction is extremely weak for the μ-atom decay process.

The spin averaged muon decay width is related to the imaginary part of the self-energy of a muon at rest in the medium. Further details and analytical expressions can be found in the Appendix of [1].

For kinematical reasons only the QE part of the W^- self-energy contributes to the muon decay. Thus, both the muon decay in the medium (Eq. (1)) and the electroweak inclusive nuclear reactions (Eq. (2)) in the QE regime are sensitive to the same physical features. We can apply the same nuclear physics corrections to the above model as in neutrino scattering, that is Pauli blocking, RPA corrections and corrections to the energy balance, see [1]. The $1s$ muon binding energy, $B_\mu^{1s} > 0$, is taken into account by replacing $m_\mu \to \hat{m}_\mu = m_\mu - B_\mu^{1s}$.

In muon capture only very small nuclear excitation energies are explored, 0–25 MeV, so the kinematical regime of the muon capture process is the worst possible for a LFG model of the nucleus. Nevertheless, the predictions of this model are in fairly good agreement with the experimental results as can be seen in Table I.

TABLE I

Experimental and theoretical total muon capture widths for different nuclei. We quote two different theoretical results: *(i)* Pauli+$\overline{Q}$: obtained without including RPA correlations, but taking into account the value of $\overline{Q}$; *(ii)* RPA: the full calculation, including all nuclear effects. Experimental data (Exp) are a weighted average: $\overline{\Gamma}/\sigma^2 = \sum_i \Gamma_i/\sigma_i^2$, with $1/\sigma^2 = \sum_i 1/\sigma_i^2$ of the results cited in [5]. Finally, in the last column we show the relative discrepancies existing between the theoretical predictions given in the third column and the experimental data of the fourth column. $\delta_{\rm rel}\Gamma = \left(\Gamma^{\rm Exp} - \Gamma^{\rm Th}\right)/\Gamma^{\rm Exp}$)

	Pauli+$\overline{Q}$ [$10^4\,s^{-1}$]	RPA [$10^4\,s^{-1}$]	Exp [$10^4\,s^{-1}$]	$\delta_{\rm rel}\Gamma$
^{12}C	5.42	3.21	3.78 ± 0.03	0.15
^{16}O	17.56	10.41	10.24 ± 0.06	−0.02
^{18}O	11.94	7.77	8.80 ± 0.15	0.12
^{23}Na	58.38	35.03	37.73 ± 0.14	0.07
^{40}Ca	465.5	257.9	252.5 ± 0.6	−0.02
^{44}Ca	318	189	179 ± 4	−0.06
^{75}As	1148	679	609±4	−0.11
^{112}Cd	1825	1078	1061±9	−0.02
^{208}Pb	1939	1310	1311±8	0.00

3. Comparison of non-correlated models

In order to simplify the calculations in the comparison between the two models we make a static approximation and expand the single nucleon weak current J^μ in the nucleon momentum keeping terms up to order zero.

In the SM we have to deal with an S matrix element of the kind

$$S_{fi} = -2\pi i \delta\left(E_f - E_i - \omega\right) \frac{G}{\sqrt{2}}\, \ell^\mu \langle f|\tilde{J}_\mu(-\boldsymbol{k}')|i\rangle\,, \tag{4}$$

where the weak current is modified to include the muon wave function

$$\tilde{J}_\mu(-\boldsymbol{k}') = \int d^3\boldsymbol{r}\, \mathrm{e}^{-i\boldsymbol{k}'\cdot\boldsymbol{r}} J_\mu(\boldsymbol{r})\phi_{1s}(\boldsymbol{r})\,. \tag{5}$$

Now the states $|i\rangle$ and $\langle f|$ are nuclear states in a shell model. This states are single particle excitations of a N nucleon system in a WS potential and can be not only in the continuum, like in a Fermi gas, but there can also be discrete excitations so we have now two contributions to the decay width.

We now have to get the nuclear wave functions as solutions of the Schrödinger equation for a WS potential where the parameters of the potential are commonly fitted to the experimental energies of the valence shells or the charge radius. In the present case of muon capture we fit the experimental Q-value for the decay reaction.

For the LFG model we use simplified expression for the decay width, where we have not taken into account RPA correlations, but energy balance and Pauli blocking effects are implemented. The only inputs remaining to be fixed are the nuclear matter densities, that will be those provided by the wave functions of the WS potential.

Up to now we have in both LFG and SM models the same physical features of Pauli blocking and correct energy balance, the only difference coming from the more refined treatment of the nuclear wave function in the SM case. In this way we can compare both SM and LFG models.

4. Results

In this section we present results for a set of closed-shell nuclei ^{12}C, ^{16}O, ^{40}Ca and ^{208}Pb. Fixing the experimental Q-value only makes one condition for fixing the several parameters of the WS potential, so wherever possible we set the remaining parameters of the potential to values similar to those used in the literature. In our calculation we use different sets of parameters, denoted WS1, WS2 and WS3. In order to compare with the LFG, we use as input the proton and neutron densities obtained in the corresponding shell model. The values of the different parameters sets can be seen in [3].

In Table II we show results for the integrated inclusive widths for the four nuclei. We can see that, in the case of WS1 and WS2, the LFG and WS results for ^{12}C are quite similar, differing only in $\sim$ 2–3%. In the case of WS3 the differences are larger, around 14%.

This can be understood in terms of the values of the parametrization WS3. For more attractive potentials the nucleus becomes more dense in the interior. For this reason, the WS3 neutron density turns out to be the smallest one, while the proton density is around 3/2 the neutron one. Therefore, a proton near the Fermi surface can decay to a neutron above the neutron

TABLE II

Integrated width in units of $10^5 s^{-1}$ for the different nuclei and Woods–Saxon potentials, compared with the LFG results using the corresponding charge densities. The discrete contribution of the shell model is shown in the first column. The column labeled % gives the relative difference between WS and LFG results.

		discrete	total	LFG	%
^{12}C	WS1	0.3115	0.4406	0.4548	3.2
	WS2	0.3179	0.4289	0.4360	1.7
	WS3	0.2746	0.5510	0.4732	−14.1
^{16}O	WS1	1.124	1.267	1.346	6.2
	WS2	0.584	1.107	1.378	24.4
	WS3	1.143	1.316	1.373	4.3
^{40}Ca	WS1	27.72	34.87	34.81	−0.1
	WS2	26.34	31.70	33.07	4.3
	WS3	24.91	30.64	33.19	8.3
^{208}Pb	WS1	128.5	191.0	187.27	−1.9
	WS2	159.6	243.4	213.64	−12.2

Fermi surface with an energy decrement. This is an unrealistic situation, since precisely in this case the neutrons are less bound than protons in the SM, and therefore, lie at higher energies. Hence the LFG results are worse for very different neutron and proton densities. Another argument to disregard this case is the well known property of closed (sub-)shell nuclei such as ^{12}C, for which the neutron and proton densities should be similar.

In Fig. 1 we compare the SM results for the differential width to the continuum with the LFG distribution for the different WS parameters (left panels). The shapes of both distributions are completely different. The partial widths to the discrete states are shown in the right panels of Fig. 1. Considering these differences in shape between the LFG and the SM, it is a very notable result that the integrated widths (adding the discrete states) take similar values in both models as was shown in Table II.

In the case of ^{16}O the integrated widths computed in the LFG are also very close, $\sim$ 4–6%, to the SM results with the potentials WS1 and WS3 (see Table II). The worst results are obtained for the WS2 parameterization; the corresponding width is 24% of the SM one. This can also been understood in terms of what was said for the case of ^{12}C above, by looking at the ^{16}O densities shown in Fig. 2.

The LFG results improve when the mass of the nucleus increases as in the case of the nucleus ^{40}Ca. In fact, from Table II we see that for this nucleus the LFG integrated width is lower than 8% for all cases. This improvement was expected because the Fermi gas description of the nucleus should work better for heavier nuclei.

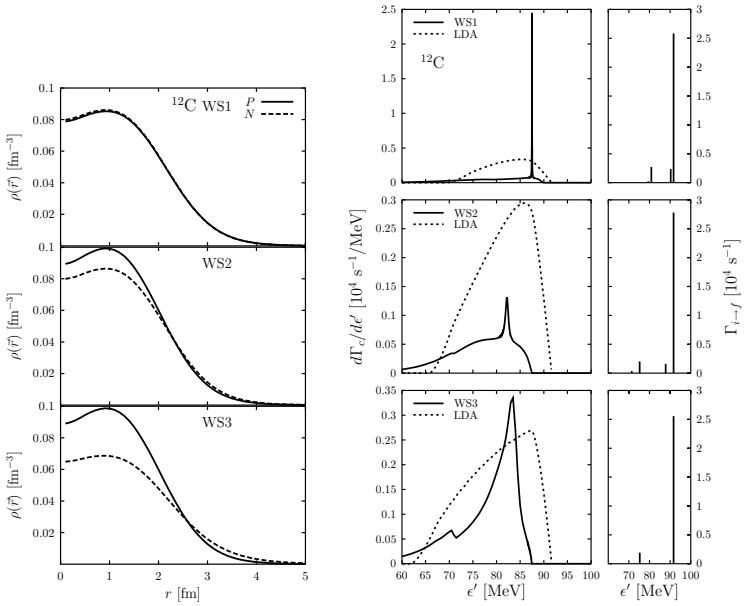

Fig. 1. The left figure shows proton and neutron densities of ^{12}C, for the several WS potentials used in this work. The right figure shows the differential SM width of ^{12}C to the continuum (left panels) compared to the LFG, and partial widths contributions to the discrete states (right panels), as a function of the neutrino energy.

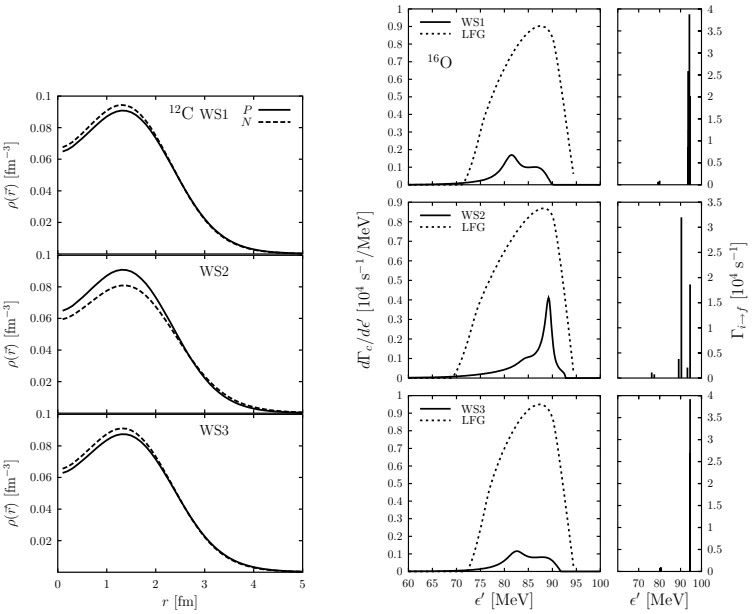

Fig. 2. The same as Fig. 1 for ^{16}O.

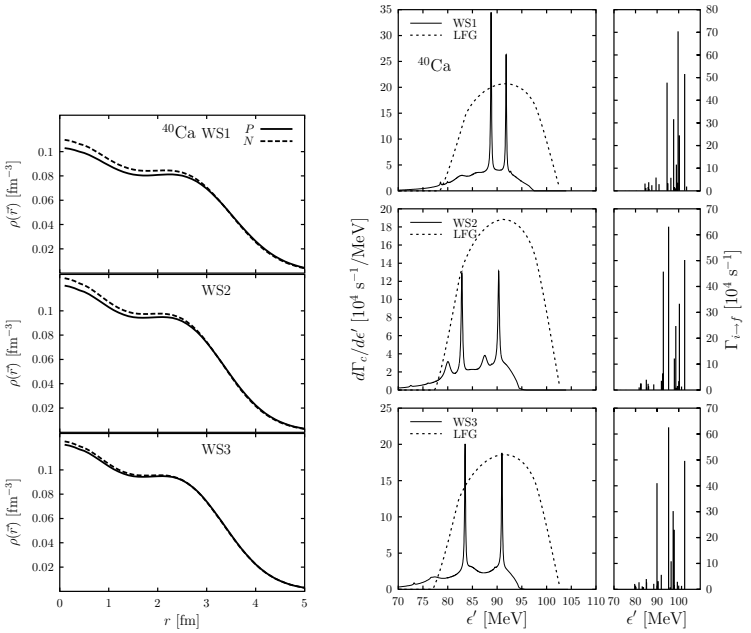

Fig. 3. The same as Fig. 1 for ^{40}Ca.

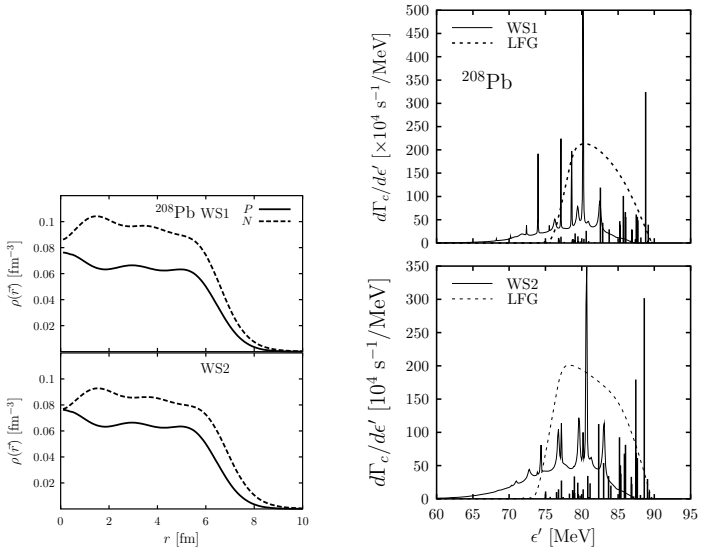

Fig. 4. The same as Fig. 1 for ^{208}Pb.

For the closed-shell heavy nucleus ^{208}Pb we present in Table II integrated widths only for two sets of potential parameters, WS1 and WS2. In both cases the LFG results are close to the SM ones.

5. Conclusions

In this paper we have estimated the magnitude of the finite nucleus effects on inclusive muon capture, aiming at quantifying the uncertainty of the LFG results of [1].

We have focused on a simple shell model without nuclear correlations, but that contains the relevant information about the finite nuclear structure, and we have compared it with the uncorrelated LFG using the same input. As expected, the neutrino spectrum is very different in the two models, in particular the LFG cannot account for the resonances and discrete states. However, in the case of the lighter nuclei, ^{12}C and ^{16}O, the SM and LFG results for the integrated width are close, within 3–6%, for WS parameters with similar neutron and proton densities. For the medium and heavy nuclei, ^{40}Ca and ^{208}Pb, the integrated widths are always very close, within 1–7%. The final neutrino spectra of the LFG become more similar to the SM, including the discrete part, for heavier nuclei.

REFERENCES

[1] J. Nieves, J.E. Amaro, M. Valverde, *Phys. Rev.* **C70**, 055503 (2004); Erratum **C72**, 019902 (2005).

[2] A. Gil, J. Nieves, E. Oset, *Nucl. Phys.* **A627**, 543 (1997); *Nucl. Phys.* **A627**, 598 (1997).

[3] J.E. Amaro, C. Maieron, J. Nieves, M. Valverde, *Eur. Phys. J.* **A24**, 343 (2005).

[4] M. Valverde, J.E. Amaro, J. Nieves, *Phys. Lett.* **B638**, 325 (2006) [hep-ph/0604042].

[5] T. Suzuki, D.F. Measday, J.P. Roalsvig, *Phys. Rev.* **C35**, 2212 (1987) and references therein.